

Effective electromechanical coupling coefficient of adaptive structures with integrated multi-functional piezoelectric structural fiber composites

Yao Koutsawa^{*1}, Sonnou Tiem², Gaetano Giunta¹ and Salim Belouettar¹

¹Centre de Recherche Public Henri Tudor, 29, Avenue John F. Kennedy, L-1855 Luxembourg, G.D. of Luxembourg

²Ecole Nationale Supérieure d'Ingénieurs, Université de Lomé, BP. 1515, Lomé, Togo

(Received March 28, 2013, Revised October 20, 2013, Accepted December 13, 2013)

Abstract. This paper presents a linear computational homogenization framework to evaluate the effective (or generalized) electromechanical coupling coefficient (EMCC) of adaptive structures with piezoelectric structural fiber (PSF) composite elements. The PSF consists of a silicon carbide (SiC) or carbon core fiber as reinforcement to a fragile piezo-ceramic shell. For the micro-scale analysis, a micromechanics model based on the variational asymptotic method for unit cell homogenization (VAMUCH) is used to evaluate the overall electromechanical properties of the PSF composites. At the macro-scale, a finite element (FE) analysis with the commercial FE code ABAQUS is performed to evaluate the effective EMCC for structures with the PSF composite patches. The EMCC is postprocessed from free-vibrations analysis under short-circuit (SC) and open-circuit (OC) electrodes of the patches. This linear two-scale computational framework may be useful for the optimal design of active structure multi-functional composites which can be used for multi-functional applications such as structural health monitoring, power harvest, vibration sensing and control, damping, and shape control through anisotropic actuation.

Keywords: smart materials; mechanical properties; electrical properties; multiscale modeling

1. Introduction

The desire to reduce the weight and complexity of systems has led to the development of new materials and structures that simultaneously perform (a) multiple structural functions, (b) combined non-structural and structural functions, or (c) both. An example of type (b) would be a load-bearing structure that has the capability of providing its own noise and vibration control, self-repair, thermal insulation, and energy harvesting/storage. Recent research on mechanics of multi-functional composite materials and structures is reviewed in Gibson (2010). For the example of type (b), Lin and Sodano developed piezoelectric structural fibers consisting of conductive structural fibers such as carbon coated with a piezoelectric interphase layer and an outer electrode layer, see Lin and Sodano (2008, 2009). Finite element (FE) models of such piezoelectric structural fiber/polymer matrix composites showed that the electromechanical coupling

*Corresponding author, Ph. D., E-mail: yao.koutsawa@tudor.lu

coefficients available from such composites can be as high as 65-70% of the corresponding coupling coefficient for the fiber itself, and that piezoelectric structural fiber (PSF) composites are suitable for vibration control, damping, energy harvesting or structural health monitoring. However, the difficulty in applying or collecting the electric fields along the piezoelectric shell of the transversely poled PSFs makes it unsuitable for autonomous sensing or actuating applications. To address this issue, very recently, it has been reported in Dai and Ng (2012) a PSF composite made by uni-directionally deploying the longitudinally poled PSFs into a polymer matrix. The proposed PSFs are fabricated by coating a piezo-ceramic onto a carbon/silicon carbide (SiC) core fiber to improve the mechanical properties of the monolithic piezoelectric material. The PSF reported in Dai and Ng (2012) was longitudinally poled along the fiber direction. Such active composite laminate with deployed PSFs is presented in Fig. 3. Micromechanics (Mori–Tanaka approach and the extended Rule of Mixture) analysis and three-dimension (3D) FE modeling were conducted in Dai and Ng (2012) to investigate the overall electromechanical properties of such PSF composites.

The advance of multi-functional composite materials requires the development of the coupled models to predict the interactions between mechanical responses and electrical fields. The increased complexity of composite structure at the micro-level greatly complicates the analysis of the structural behavior, which is necessary for the rational design of these structures. If one is interested in capturing the effect of the micro-scale response (fluctuation) on the system response, direct analysis of such structures using standard numerical methods (e.g., FE method), although possible, is computationally intensive and unrealistic. Alternatively, one can look for effective property estimation of these multi-functional materials and then use them judiciously to have an estimate of the average response. This approach is computationally many orders of magnitude more efficient in capturing the average response and the micro-scale response (fluctuation) can be obtained from the macro-scale response with minimal computational effort.

Over the last 50 years, numerous micromechanics models have been proposed to predict the effective properties of composite materials from known constituents informations (e.g., properties, topology and morphology textures). Roughly, the micromechanics models for composite materials can be classified in two categories: (a) mean field (MF)-based models and (b) local field (LF)-based models. The MF-based methods, see Qu and Cherkaoui (2006), are based on Eshelby's solutions, see Eshelby (1957), and are capable of predicting the entire behavior of composite materials under arbitrary loads. They can provide reasonable estimates for a material's bulk elastic response but typically fail to provide good estimates for the local responses and the history-dependent responses of the material. They use averaged representations of the local fields within the constituents of the composite, i.e., they do not account for the local fluctuations of the field quantities. In order to correctly predict the local and bulk response characteristics in the elastic and inelastic domains, LF-based micromechanical theories consider both the average fields within phases as well as the fluctuating fields within the phases. There are a number of such theories currently available, see Yu *et al.* (2007) and references cited therein.

The purpose of this work is two-fold. First, the effective electromechanical properties of the PSF composites reported in Dai and Ng (2012) will be investigated using the Variational Asymptotic Method for Unit Cell Homogenization (VAMUCH), a recently developed micromechanics modeling framework, see Yu and Tang (2007), Tang and Yu (2008), Koutsawa *et al.* (2012). This method is based on the variational asymptotic method (VAM), see Berdichevsky (1977, 1979), which is applicable to any solid mechanics problem admitting a variational structure where one or more relatively small parameters are involved. The “smallness” of these parameters

is exploited by using an asymptotic expansion structure of the functional of the problem (and not of the unknown field quantities as done in the traditional asymptotic methods). The VAM combines the advantages of both variational (most notably FE structure) and asymptotic methods. With the VAMUCH, a two-dimension (2D) unit cell (UC) is sufficient to predict the full 3D anisotropic overall electromechanical properties of a PSF composite instead of 3D UCs used in Dai and Ng (2012).

Second, the effective electromechanical properties of the PSF composite will be used in a FE model to evaluate the effective (or generalized) electromechanical coupling coefficient (EMCC) for structures with integrated PSF composites elements. The EMCC measures the energy conversion efficiency of a piezo-ceramic material. The EMCC is an important measure of the effectiveness of the electromechanical coupling and, thus, of the effectiveness of a piezoelectric material for a given application. The EMCC has been used as an important parameter for several applications, such as passive shunt damping, active control authority improvement, piezoelectric power harvesting and damage detection. Some authors have used the EMCC as index or objective function in the design, positioning and sizing optimization of piezoelectric transducers, see Trindade and Benjeddou (2009) and references cited therein.

The paper is organized as follows. Section 2 briefly presents the main ingredients of the VAMUCH approach specified for the micromechanical analysis of continuous PSF composites. Section 3 describes the FE modeling using the commercial FE code ABAQUS to evaluate the effective EMCC for mechanical structure with bonded PSF composite patches. The main results regarding the two objectives of this work are presented and discussed in Section 4. Conclusions are drawn in Section 5.

2. Variational asymptotic method for heterogeneous piezoelectric materials

The general VAMUCH theory in Tang and Yu (2008), Koutsawa *et al.* (2012) can be specified for the micromechanical analysis of continuous PSF composites as the minimization of the following functional

$$\Pi = \langle C_{i\alpha j\beta} (\bar{\epsilon}_{i\alpha} + \chi_{\alpha,i})(\bar{\epsilon}_{j\beta} + \chi_{\beta,j}) \rangle \quad (1)$$

subject to the following constraints

$$\chi_{\alpha} \left(\mathbf{x}; y_1, y_2 = -\frac{d_2}{2}, y_3 \right) = \chi_{\alpha} \left(\mathbf{x}; y_1, y_2 = +\frac{d_2}{2}, y_3 \right) \quad (2)$$

$$\chi_{\alpha} \left(\mathbf{x}; y_1, y_2, y_3 = -\frac{d_3}{2} \right) = \chi_{\alpha} \left(\mathbf{x}; y_1, y_2, y_3 = +\frac{d_3}{2} \right) \quad (3)$$

$$\langle \chi_{\alpha} \rangle = 0 \quad (4)$$

Π is minimized with respect to χ_{α} . Here the angle brackets denote averaging over the UC, $C_{i\alpha j\beta}$ the positionally dependent fourth-order electro-elasticity tensor, $\bar{\epsilon}_{i\alpha}$ contains both the 3D macroscopic strain field ($\bar{\epsilon}_{ij}$) and the 3D macroscopic electric field (\bar{E}_i), χ_{α} the fluctuating functions, $\chi_{\alpha,j} = \partial\chi_{\alpha}/\partial y_j$, y_i the Cartesian coordinates describing the UC with y_2 and y_3 originated from the middle of the UC, and d_2 and d_3 the UC lengths in y_2 and y_3 directions

respectively, see Fig. 1. Throughout this paper, Latin indices are space indices assuming the values 1 to 3 while and Greek indices are fields indices assuming the values 1 to 4 and repeated indices are summed over their range except where explicitly indicated. The VAMUCH formulation uses three coordinates systems: two cartesian coordinates $\mathbf{x} = (x_1, x_2, x_3)$ and $\mathbf{y} = (y_1, y_2, y_3)$ and an integer-valued coordinate $\mathbf{n} = (n_1, n_2, n_3)$, see Fig. 1. x_i are used as the global coordinates to describe the macroscopic structure and y_i parallel to x_i as the local coordinates to describe the UC. To uniquely locate a UC in the heterogeneous material, the integer coordinates n_i is introduced. The integer coordinates are related to the global coordinates in such a way that $n_i = x_i/d_i$. Let us denote by $v_i(\mathbf{x})$ and $\psi(\mathbf{x})$ the macroscopic displacements and electric potential fields, respectively. If we denote by $u_i(\mathbf{x}; \mathbf{y})$ and $\phi(\mathbf{x}; \mathbf{y})$ the displacements and electric potential fields within the UC, respectively, then the fluctuation functions, $\chi_\alpha(\mathbf{x}; \mathbf{y})$, are defined as follows, see Tang and Yu (2008) for more details

$$u_i(\mathbf{x}; \mathbf{y}) = v_i(\mathbf{x}) + y_j \frac{\partial v_i(\mathbf{x})}{\partial x_j} + \chi_i(\mathbf{x}; \mathbf{y}) \tag{5}$$

$$\phi(\mathbf{x}; \mathbf{y}) = \psi(\mathbf{x}) + y_i \frac{\partial \psi(\mathbf{x})}{\partial x_i} + \chi_4(\mathbf{x}; \mathbf{y}) \tag{6}$$

Eqs. (2) and (3) express the traditional periodic boundary conditions at $(y_2 = -d_2/2, y_2 = +d_2/2)$ and $(y_3 = -d_3/2, y_3 = +d_3/2)$ respectively. As it is shown in Tang and Yu (2008), Eq. (4) does not affect the minimum value of the functional in Eq. (1) but helps uniquely to determine the fluctuating functions, χ_α . Here it is assumed that the PSF axis is parallel to the y_1 -axis. Therefore, the partial derivatives of the fluctuating functions, $\chi_{\alpha,1}$, will vanish because the PSF composite is uniform in the y_1 direction. At this point it is important to precise that $\bar{\epsilon}_{ij}(\mathbf{x}) = (v_{i,j} + v_{j,i})/2$ and $\bar{\epsilon}_{i4}(\mathbf{x}) = \bar{E}_i(\mathbf{x}) = -\psi_{,i}$.

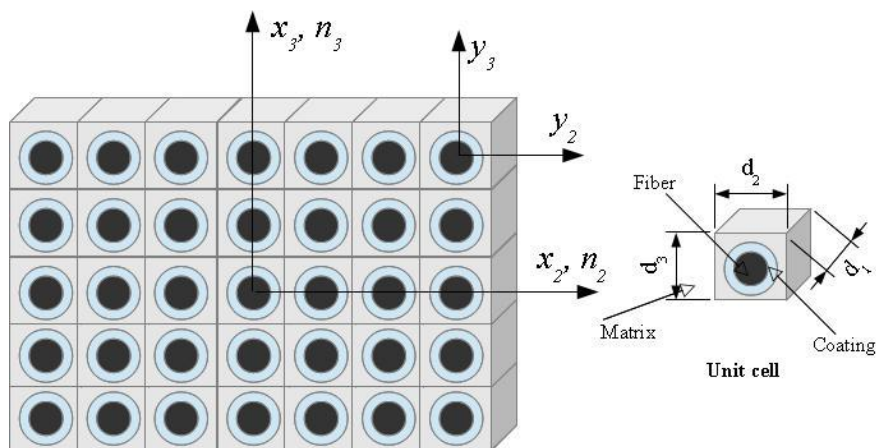


Fig. 1 Coordinate systems for periodic heterogeneous materials and the corresponding unit cell

The functional (1) can be restated in a matrix form as minimizing the following functional

$$\Pi = \frac{1}{\Omega} \int_{\Omega} \{\bar{\epsilon}(\mathbf{x}) + \epsilon(\mathbf{x}; \mathbf{y})\}^T [\mathbf{D}] \{\bar{\epsilon}(\mathbf{x}) + \epsilon(\mathbf{x}; \mathbf{y})\} d\Omega \tag{7}$$

where

$$\epsilon(\mathbf{x}; \mathbf{y}) = \begin{bmatrix} 0 & 0 & 0 & 0 \\ 0 & \frac{\partial}{\partial y_2} & 0 & 0 \\ 0 & 0 & \frac{\partial}{\partial y_3} & 0 \\ 0 & \frac{\partial}{\partial y_3} & \frac{\partial}{\partial y_2} & 0 \\ \frac{\partial}{\partial y_3} & 0 & 0 & 0 \\ \frac{\partial}{\partial y_2} & 0 & 0 & 0 \\ 0 & 0 & 0 & 0 \\ 0 & 0 & 0 & -\frac{\partial}{\partial y_2} \\ 0 & 0 & 0 & -\frac{\partial}{\partial y_3} \end{bmatrix} \begin{Bmatrix} \chi_1 \\ \chi_2 \\ \chi_3 \\ \chi_4 \end{Bmatrix} = \mathcal{H}\chi(\mathbf{x}; \mathbf{y}) \tag{8}$$

$[\mathbf{D}]$ is the 9×9 material matrix condensed from the positionally dependent fourth-order electro-elasticity tensor, $C_{i\alpha j\beta}$, Ω is the area of the UC. The matrix $[\mathbf{D}]$ includes the elastic (\mathbf{C}), piezoelectric (\mathbf{e}), and dielectric ($\boldsymbol{\kappa}$) properties and is expressed as

$$[\mathbf{D}] = \begin{bmatrix} \mathbf{C} & -\mathbf{e}^T \\ -\mathbf{e} & -\boldsymbol{\kappa} \end{bmatrix} \tag{9}$$

If one discretizes χ using the finite elements as

$$\chi(\mathbf{x}; \mathbf{y}) = \mathbf{S}(y_2, y_3)\Gamma(\mathbf{x}) \tag{10}$$

where $\mathbf{S}(y_2, y_3)$ representing the shape functions (in the assembled sense) and $\Gamma(\mathbf{x})$ a column matrix of the nodal field variables of the fluctuation functions (considering the constraints (2) and (3)), one obtains a discretized version of the functional as

$$\Pi = \frac{1}{\Omega} (\Gamma^T \mathbf{D}_{\chi\chi} \Gamma + 2\Gamma^T \mathbf{D}_{\chi\epsilon} \bar{\epsilon} + \bar{\epsilon}^T \mathbf{D}_{\epsilon\epsilon} \bar{\epsilon}), \tag{11}$$

where

$$\mathbf{D}_{\chi\chi} = \int_{\Omega} [\mathcal{H}\mathbf{S}]^T [\mathbf{D}][\mathcal{H}\mathbf{S}] d\Omega \tag{12}$$

$$\mathbf{D}_{\chi\varepsilon} = \int_{\Omega} [\mathcal{H}\mathcal{S}]^T [\mathbf{D}] d\Omega \quad (13)$$

$$\mathbf{D}_{\varepsilon\varepsilon} = \int_{\Omega} [\mathbf{D}] d\Omega \quad (14)$$

From now on, for simplicity, $\Gamma(\mathbf{x})$ is replaced by Γ . The minimization of Eq. (11) with respect to Γ gives the following linear system

$$\mathbf{D}_{\chi\chi} \Gamma = -\mathbf{D}_{\chi\varepsilon} \bar{\varepsilon} \quad (15)$$

The solution of Eq. (15) can be written as

$$\Gamma(\mathbf{x}) = \Gamma_0 \bar{\varepsilon}(\mathbf{x}), \quad (16)$$

where Γ_0 is the solution of the linear system

$$\mathbf{D}_{\chi\chi} \Gamma_0 = -\mathbf{D}_{\chi\varepsilon}. \quad (17)$$

Here, the linear system (17) is solved using the multifrontal massively parallel sparse direct solver (MUMPS), see Amestoy *et al.* (2001, 2006), within the GetFEM++ FE library, see Renard and Pommier (2011). Substituting Eq. (16) into Eq. (11), one can calculate the electric enthalpy of the UC as

$$\Pi = \frac{1}{\Omega} \bar{\varepsilon}^T (\Gamma_0^T \mathbf{D}_{\chi\varepsilon} + \mathbf{D}_{\varepsilon\varepsilon}) \bar{\varepsilon} \equiv \bar{\varepsilon}^T \bar{\mathbf{D}} \bar{\varepsilon}, \quad (18)$$

where $\bar{\mathbf{D}}$ is the effective (or homogenized) piezoelectric material matrix which can be expressed using a 9×9 matrix as

$$\bar{\mathbf{D}} = \frac{\partial^2 \Pi}{\partial \bar{\varepsilon} \partial \bar{\varepsilon}} = \begin{bmatrix} \bar{\mathbf{C}} & -\bar{\mathbf{e}}^T \\ -\bar{\mathbf{e}} & -\bar{\kappa} \end{bmatrix}. \quad (19)$$

Having obtained the effective electro-elastic properties, one can use these properties to carry out the macroscopic analysis of the complete structure to predict the global electro-elastic behavior of the engineering system integrating the PSF composite. If one needs the point-wise distribution of the electro-elastic fields (displacements, strains, stresses, electric potential, etc.) within the microstructure, one has to uniquely determine the fluctuation functions, χ_α , using the constraints in Eq. (4) and follow the recovery procedure explained in Tang and Yu (2008). Although it is easy to distinguish the VAMUCH from other analytical micromechanics approaches, the VAMUCH is often confused as one of the finite element analysis (FEA)-based micromechanics approaches because the equations of the VAMUCH theory are solved using the FE technique. FEA-based micromechanics approaches carry out a conventional FEA of a UC with specially designed boundary conditions under specifically designed loads (see Dai and Ng (2012), for example).

3. Effective EMCC for mechanical structure with bonded PSF composite patches

The EMCC measures the energy conversion efficiency of a piezo-ceramic material. Several formulas and methods were proposed to evaluate numerically or measure experimentally the EMCC of a piezoelectric material, see Chevallier *et al.* (2008, 2009), Trindade and Benjeddou (2009) for more details. The technique for evaluating the effective EMCC based on the

short-circuit (SC) and open-circuit (OC) eigen-frequencies presented in Chevallier *et al.* (2008, 2009) is applied here to elastic beams with PSF composite patches. The modal effective EMCC is post-processed from free vibrations analysis under SC and OC electrodes of the patches. Hence, two cantilever Aluminium beams with symmetrically bonded PSF composite patches, having the same poling (SP) directions, were analyzed in free-vibrations for SC and OC electrodes with equipotential (EP) constraints. The effective square EMCC for the structure with piezoelectric elements, vibrating in the i -th mode, can be defined as (see Chevallier *et al.* (2008, 2009))

$$K_i^2 = \frac{f_{i,OC}^2 - f_{i,SC}^2}{f_{i,SC}^2}, \quad (20)$$

where f_i is the natural frequency of the i -th mode. The free-vibrations analysis of the cantilever beams were performed here using ABAQUS FE commercial codes. The cantilever adaptive beam has been discretized using quadratic (20-nodes) brick elements. C3D20R (R for reduced integration) and C3D20ER (E for electric) were used for the Aluminium beam and the PSF composite patches, respectively (see Fig. 2(b)).

For the SC condition, the patches four faces are selected and a nil potential is applied on them. For the OC case, the faces of the patches are charge free. The usual way is to not apply any electric condition. However, for physical reasons, the EP condition has to be added by coupling the nodes of each face of the patches, see Chevallier *et al.* (2008, 2009). The EP constraints of the patches surfaces are expressed by the following relationships used between the electric DOFs (DOF 9 in ABAQUS)

*EQUATION

2

SP1EXT, 9, 1.0, NP1EXT, 9, -1.0

2

SP1INT, 9, 1.0, NP1INT, 9, -1.0

2

SP2EXT, 9, 1.0, NP2EXT, 9, -1.0

2

SP2INT, 9, 1.0, NP2INT, 9, -1.0

where

- SP1EXT is a set of all nodes of the PSF patch 1 external surface except a node,
- NP1EXT is the remaining node of the PSF patch 1 external surface,
- SP1INT is a set of all nodes of the PSF patch 1 internal surface except a node,
- NP1INT is the remaining node of the PSF patch 1 internal surface,
- SP2EXT is a set of all nodes of the PSF patch 2 external surface except a node,
- NP2EXT is the remaining node of the PSF patch 2 external surface,
- SP2INT is a set of all nodes of the PSF patch 2 internal surface except a node,
- NP2INT is the remaining node of the PSF patch 2 internal surface.

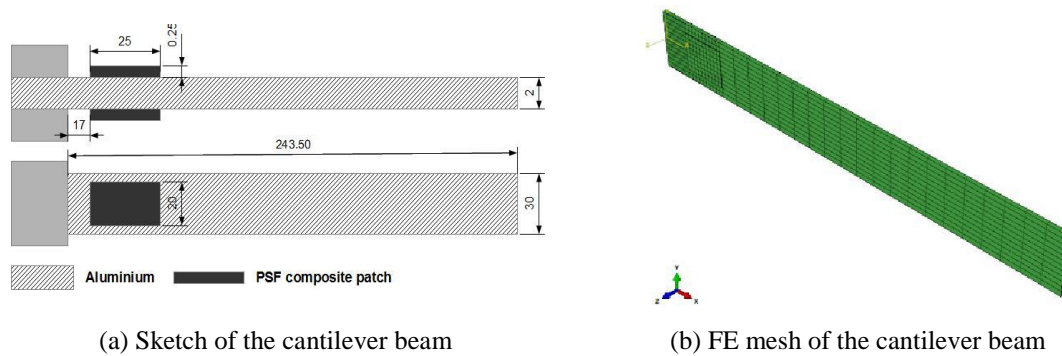


Fig. 2 Cantilever beam with a bonded pair of PSF composite patches (dimensions in mm).

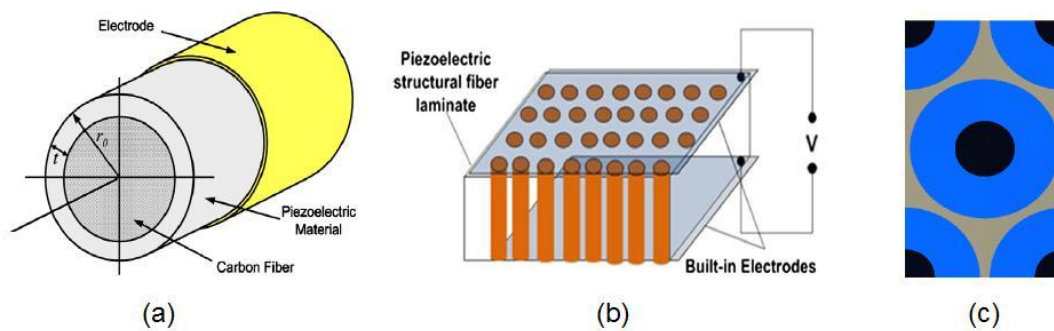


Fig. 3 Piezoelectric structural fiber (PSF) composites, (a) structure of one PSF (Lin and Sodano 2008) (b) PSF laminate with built-in electrodes (Dai and Ng 2012) and (c) representative volume element (RVE) of the PSF composites with hexagonal packing

4. Results and discussion

In the following sections, the main results concerning the effective electromechanical properties of the PSF composite and their EMCC via free-vibrations analysis are presented and discussed.

4.1 Effective electro-elastic properties of a PSF composite

In this section, the electro-elastic properties of a PSF composite (see Fig. 3(b)) are predicted using the VAMUCH micromechanics approach described in Section 2. Hexagonal packing of the PSFs is assumed, see Fig. 3(c).

The constituents' materials properties of the PSF composite are presented in Tables 1 and 2.

Table 1 Material mechanical properties of the constituent phases of the PSF composite

| Material | C_{11} | C_{12} | C_{13} | C_{23} | C_{33} | C_{44} | C_{66} | ρ |
|----------|----------|----------|----------|----------|----------|----------|----------|----------------------|
| | [GPa] | [kg/m ³] |
| Epoxy | 8 | 4.4 | 4.4 | 4.4 | 8 | 1.8 | 1.8 | 1300 |
| Carbon | 24 | 9.7 | 6.7 | 6.7 | 250 | 27 | 11 | 2200 |
| PIC255 | 105.2 | 58.3 | 55.4 | 55.4 | 85.9 | 21 | 23.5 | 7800 |

Table 2 Material piezo-electric and dielectric properties of the constituent phases of the PSF composite

| Material | e_{31} | e_{32} | e_{33} | e_{15} | e_{24} | κ_{11}/k_0^1 | κ_{22}/k_0 | κ_{33}/k_0 |
|----------|---------------------|---------------------|---------------------|---------------------|---------------------|---------------------|-------------------|-------------------|
| | [C/m ²] | - | - | - |
| Epoxy | - | - | - | - | - | 4 | 4 | 4 |
| Carbon | - | - | - | - | - | 12 | 12 | 12 |
| PIC255 | -7.25 | -7.25 | 14.41 | 11.57 | 11.57 | 931.22 | 931.22 | 804.38 |

¹: 8.8510^{-12} C/Vm.

In what follows, the aspect ratio, α , of the PSF is defined as the value of the coating thickness, t , divided by the outer radius, r_0 , as shown in Fig. 3(a). It is worth noting that VAMUCH has been extensively validated against 3D FE-based micromechanics models, see Tang and Yu (2008), Koutsawa *et al.* (2012). In this work, our implementation has been validated against 3D FE modeling using ANSYS following the procedure reported in Koutsawa *et al.* (2010). It has been found that the 2D VAMUCH and the 3D ANSYS predictions match very well for all the considered volume fractions and aspect ratios for the PSF.

Figs. 4(a) and 4(b) show the variation of the effective elastic coefficients \bar{C}_{11} and \bar{C}_{33} of the PSF composite with the PSF volume fraction (v_{PSF}) and α . For all aspect ratios, a linear variation of the longitudinal elastic coefficient, \bar{C}_{33} , with v_{PSF} is observed while the transverse elastic coefficient, \bar{C}_{11} , is an exponential function of v_{PSF} . The PSF composite with a larger volume of piezoelectric material has higher transverse modulus. This is explained by the high C_{11} modulus of the piezoelectric material (PIC255), see Table 1. Since the C_{33} modulus of PIC255 is less than that of the Carbon fiber, it is expected that the PSF composite with a larger volume of piezoelectric material has smaller longitudinal modulus, see Fig. 4(b).

Figs. 5(a) and 5(b) show the variation of the effective elastic coefficients \bar{C}_{12} and \bar{C}_{23} of the PSF composite with v_{PSF} and α . Both effective elastic coefficients are exponential functions of v_{PSF} . As it is expected from the C_{12} and C_{23} coefficients (see Table 1), the PSF composite with a larger volume of piezoelectric material has higher \bar{C}_{12} and \bar{C}_{23} coefficients.

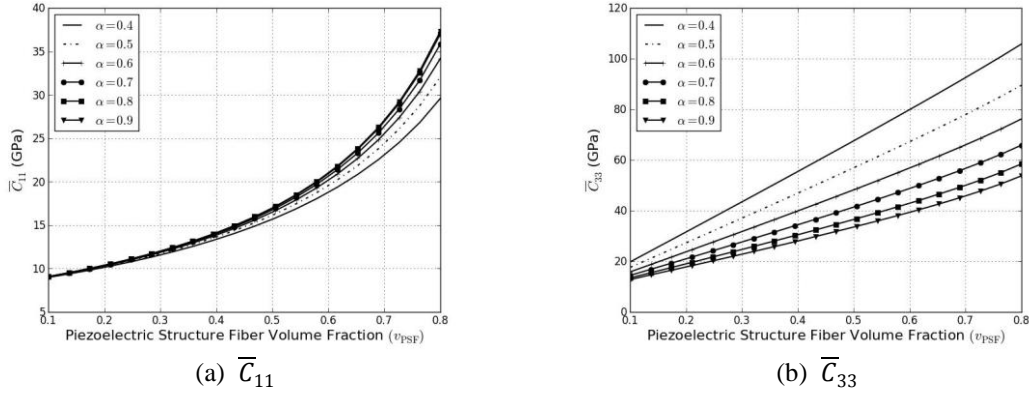


Fig. 4 Variation of the effective elastic coefficients \bar{C}_{11} and \bar{C}_{33} of the PSF composite with the PSF volume fraction and aspect ratio, α

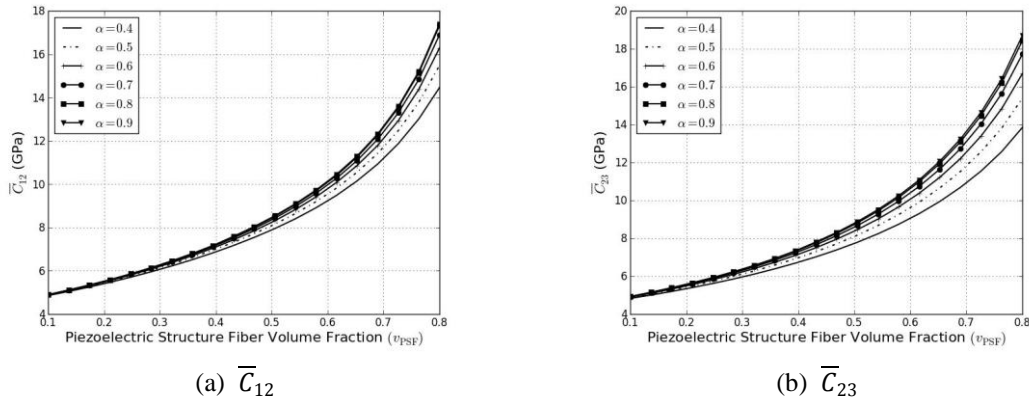


Fig. 5 Variation of the effective elastic coefficients \bar{C}_{12} and \bar{C}_{23} of the PSF composite with the PSF volume fraction and aspect ratio, α

Figs. 6(a) and 6(b) show the variation of the effective elastic shear coefficients \bar{C}_{66} and \bar{C}_{55} of the PSF composite with v_{PSF} and α . Both effective elastic shear coefficients are exponential functions of v_{PSF} . In general, the predicted effective elastic shear coefficients are not highly sensitive to α . The transverse effective elastic shear coefficient, \bar{C}_{66} , is more sensitive to α for high values of v_{PSF} while \bar{C}_{55} is quite insensitive to α .

The functionality of the PSF composites is due to the piezoelectric phase since these materials have relatively high dielectric constant and piezoelectric coupling coefficient while the flexibility and the strength of the PSF composites are due to the polymer matrix and the carbon fiber respectively. Figs. 7(a) and 7(b) show the variation of the effective dielectric coefficients $\bar{\kappa}_{11}$ and $\bar{\kappa}_{33}$ of the PSF composite with v_{tPSF} and α . The predicted transverse permittivity (Fig. 7(a))

shows an exponential increase with respect to v_{PSF} while the longitudinal permittivity (Fig. 7(b)) has a linear relationship. The transverse permittivity, $\bar{\kappa}_{11}$, is quite insensitive to α . Figs. 8(a)- 8(c) show the variation of the effective piezoelectric coefficients \bar{e}_{15} , \bar{e}_{31} and \bar{e}_{33} of the PSF composite with v_{PSF} and α . \bar{e}_{15} , \bar{e}_{31} show an exponential increase with respect to v_{PSF} while \bar{e}_{33} has a linear relationship. \bar{e}_{15} is insensitive to α while the PSF composite with a larger volume of piezoelectric material has higher \bar{e}_{31} and \bar{e}_{33} . It is worth mentioning that for $v_{\text{PSF}} = 0.8$ and $\alpha = 0.9$, $\bar{e}_{33} = 13.82$ which is about 95% of $e_{33} = 14.41$ of the piezoelectric (PIC255) phase.

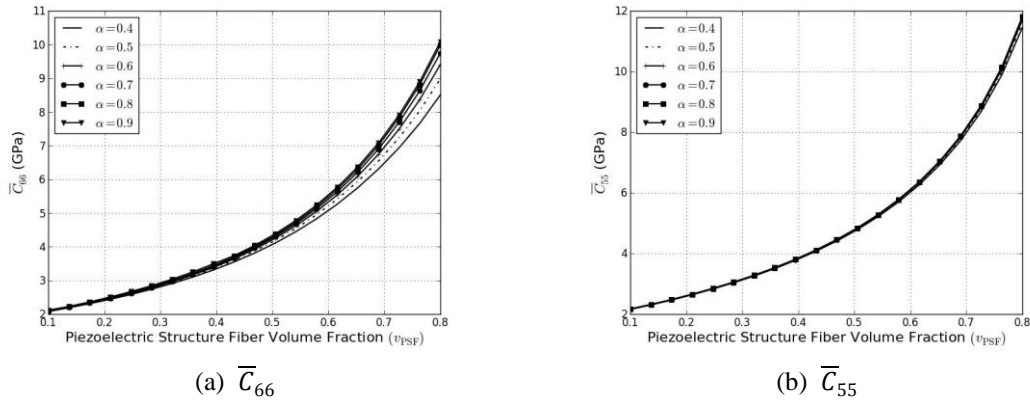


Fig. 6 Variation of the effective elastic coefficients \bar{C}_{66} and \bar{C}_{55} of the PSF composite with the PSF volume fraction and aspect ratio, α

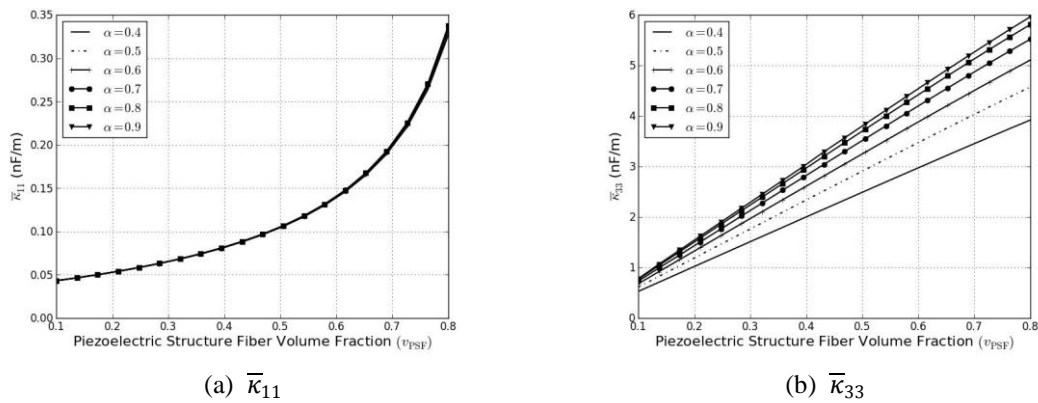


Fig. 7 Variation of the effective dielectric properties $\bar{\kappa}_{11}$ and $\bar{\kappa}_{33}$ of the PSF composite with the PSF volume fraction and aspect ratio, α

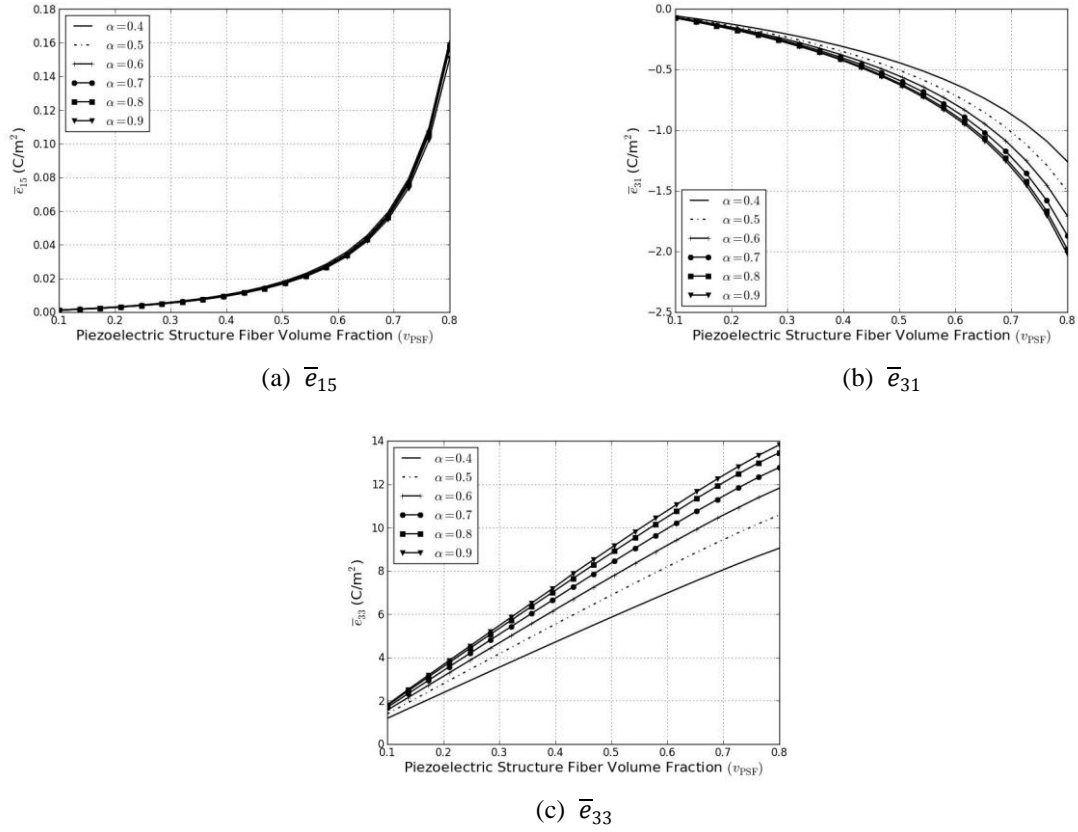


Fig. 8 Variation of the effective piezoelectric properties \bar{e}_{15} , \bar{e}_{31} and \bar{e}_{33} of the PSF composite with the PSF volume fraction and aspect ratio, α

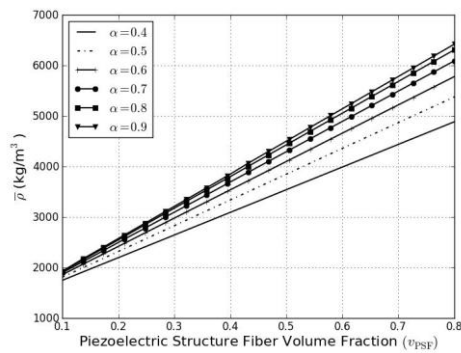


Fig. 9 Variation of the effective density $\bar{\rho}$ of the PSF composite with the PSF volume fraction and aspect ratio, α

Fig. 9 shows the variation of the effective density, $\bar{\rho}$, of the PSF composite with v_{PSF} and α . Here, $\bar{\rho}$ is predicted by a volume averaging over the volume of the PSF composite UC

$$\bar{\rho} = \frac{1}{\Omega} \int_{\Omega} \rho \, d\Omega \quad (21)$$

A linear variation of $\bar{\rho}$ with v_{PSF} is observed and as it is expected (see Table 1), the PSF composite with a larger volume of piezoelectric material has higher effective density.

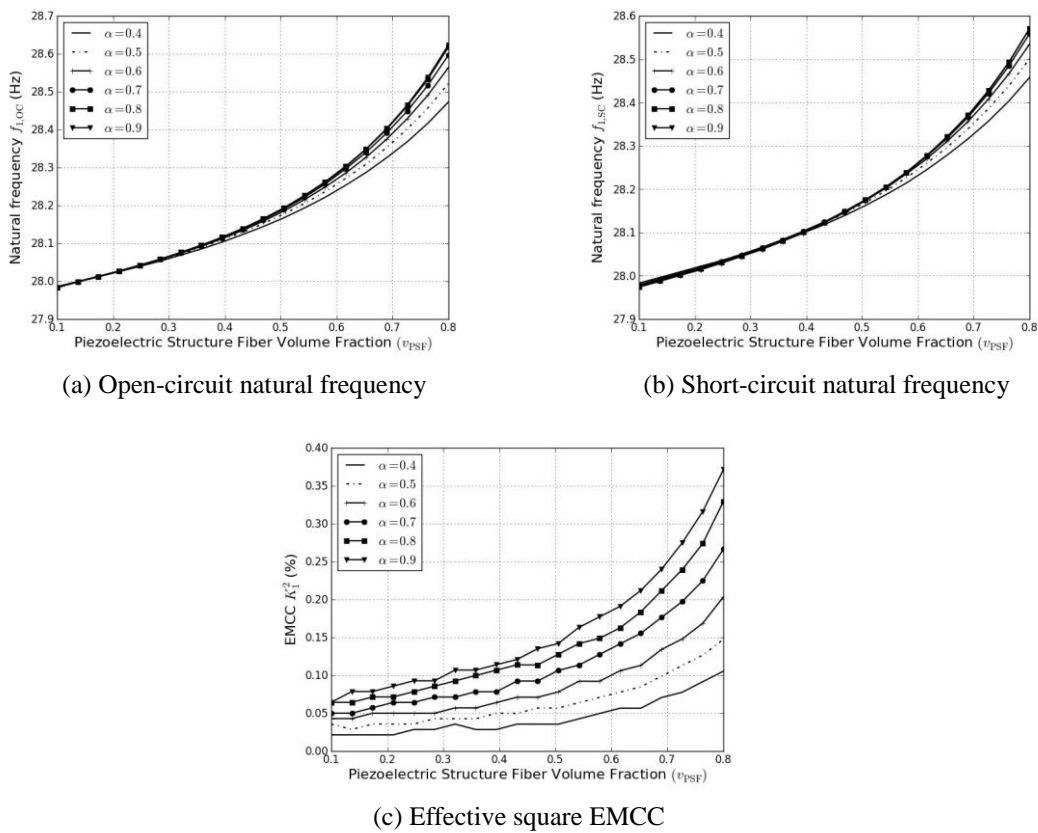


Fig. 10 Variation of the natural frequencies $f_{1,OC}$ and $f_{1,SC}$ and the square EMCC K_1^2 of the cantilever beam with the PSF volume fraction and aspect ratio, α

4.2. Evaluation of the EMCC

The cantilever beam presented in Fig. 2 is used to evaluate the EMCC. The beam has a length of 243.5 mm, a thickness of 2 mm and a width of 30 mm, and its material properties are: Young modulus 69 GPa, mass density 2700 kg m^{-3} and Poisson ratio 0.3.

Figs. 10(a) and 10(b) show the variation of the natural frequencies of the cantilever beam with the PSF composite patches under the OC and SC boundary conditions for the first free-vibrations

mode. The natural frequency is sensitive to α for high values of v_{PSF} . PSF composite patch with a larger volume of piezoelectric material gives higher natural frequency. As discussed in Chevallier *et al.* (2008), OC and SC configurations yield very close results. Nevertheless the small difference is of paramount importance since it is a measure of the electro-mechanical coupling capability of the structure. Hence, the variation of the square EMCC (see Eq. (20)) is shown by Fig. 10(c). The EMCC is sensitive to the aspect ratio, α . The PSF composite patches with a larger volume of piezoelectric material has higher square EMCC. Similar results are observed for the second vibration mode of the smart cantilever beam. The first and second vibration modes are out-of-plane bending modes. For the third (in-plane bending) and fourth (torsion) modes, the application of the EP constraint make their electrode potential distribution average nil leading to identical SC and OC frequencies, hence a nil EMCC. The third and fourth modes become uncoupled when the EP is applied because their potential distributions are unsymmetric. These results are not reported here for brevity.

5. Conclusions

This work presents a linear computational homogenization framework to evaluate the energy conversion efficiency of a piezoelectric structural fiber (PSF) composite for multi-functional applications. The PSFs are composed of a carbon/SiC core fiber and a piezo-ceramic coating and are deployed unidirectionally into a polymer matrix. At the micro-scale, the electromechanical properties of piezoelectric structural fiber composites are predicted by the variational asymptotic method for unit cell homogenization (VAMUCH) micromechanics approach. With the VAMUCH, a two-dimension unit cell is sufficient to predict the full three-dimension anisotropic effective electromechanical properties of the PSF composite. Having obtained these effective electromechanical properties, a free-vibrations analysis (macro-scale) has been performed on a cantilever beam with a single pair of patches made by PSF composite. The free-vibrations analysis has been done under short-circuit and open-circuit conditions using the commercial FE codes ABAQUS. The electromechanical coupling coefficient (EMCC) is post-processed from these free-vibrations analysis. The results show that the EMCC is sensitive to the aspect ratio of the PSF. The PSF composite patches with a larger volume of piezoelectric material have higher EMCC. The proposed linear computational homogenization framework may be useful for the optimal design of active structure multi-functional composites which can be used for multi-functional applications such as structural health monitoring, power harvest, vibration sensing and control, damping, and shape control through anisotropic actuation.

Acknowledgments

This study is supported by the Fonds National de la Recherche Luxembourg (FNR) under the CORE projects C10/MS/787395-ASPIEZO and C09/MS/05 FUNCTIONALLY.

References

- Amestoy, P.R., Duff, I.S., Koster, J. and L'Excellent, J.Y. (2001), "A fully asynchronous multifrontal solver using distributed dynamic scheduling", *SIAM J. Matrix Anal. A.*, **23**(1), 15-41.
- Amestoy, P.R., Guermouche, A., L'Excellent, J.Y. and Pralet, S. (2006), "Hybrid scheduling for the parallel solution of linear systems", *Parallel Comput.*, **32**(2), 136-156.
- Berdichevsky, V. (1977), "On averaging of periodic systems", *Prikl. Mat. Mekh.*, **41**(6), 993-1006.
- Berdichevsky, V. (1979), "Variational-asymptotic method of constructing a theory of shells", *Prikl. Mat. Mekh.*, **43**(4), 664-687.
- Chevallier, G., Ghorbel, S. and Benjeddou, A. (2008), "A benchmark for free vibration and effective coupling of thick piezoelectric smart structures", *Smart Mater. Struct.*, **17**(6), 065007(11pp).
- Chevallier, G., Ghorbel, S. and Benjeddou, A. (2009), "Piezoceramic shunted damping concept: testing, modelling and correlation", *Mecaniqueet Industries*, **10**(5), 397-411.
- Dai, Q. and Ng, K. (2012), "Investigation of electromechanical properties of piezoelectric structural fiber composites with micromechanics analysis and finite element modeling", *Mech. Mater.*, **53**, 29- 46.
- Eshelby, J. (1957), "The determination of the elastic field of an ellipsoidal inclusion and related problems", *Proc. Roy. Soc. A*, **241**, 376-396.
- Gibson, R.F. (2010), "A review of recent research on mechanics of multifunctional composite materials and structures", *Compos. Struct.*, **92**(12), 2793- 2810.
- Koutsawa, Y., Belouettar, S., Makradi, A. and Tiem, S. (2012), "X-FEM implementation of VAMUCH: application to active structural fiber multi-functional composite materials", *Compos. Struct.*, **94**(4), 1297 -1304.
- Koutsawa, Y., Biscani, F., Belouettar, S., Houssein, N. and Carrera, E. (2010), "Multi-coating in homogeneities approach for the effective thermo-electro-elastic properties of piezoelectric composite materials", *Compos. Struct.*, **92**(4), 964-972.
- Lin, Y. and Sodano, H.A. (2008), "Concept and model of a piezoelectric structural fiber for multifunctional composites", *Compos. Sci. Technol.*, **68**(7-8), 1911 - 1918.
- Lin, Y. and Sodano, H.A. (2009), "Electromechanical characterization of a active structural fiber lamina for multifunctional composites", *Compos. Sci. Technol.*, **69**(11-12), 1825 –1830. Experimental Techniques and Design in Composite Materials (ETDCM8) with Regular Papers.
- Qu, J. and Cherkaoui, M. (2006), *Fundamentals of micromechanics of solids*, John Wiley & Sons, Inc., Hoboken, New Jersey.
- Renard, Y. and Pommier, J. (2011), GetFEM++: An open-source finite element library.
- Tang, T. and Yu, W. (2008), "Variational asymptotic micromechanics modeling of heterogeneous piezoelectric materials", *Mech. Mater.*, **40**(10), 812- 824.
- Trindade, M. and Benjeddou, A. (2009), "Effective electromechanical coupling coefficients of piezoelectric adaptive structures: Critical evaluation and optimization", *Mech. Adv. Mater. Struct.*, **16**(3), 210-223.
- Yu, W. and Tang, T. (2007), "Variational asymptotic method for unit cell homogenization of periodically heterogeneous materials", *Int. J. Solids Struct.*, **44**(11-12), 3738 -3755.
- Yu, W., Williams, T.O., Bednarczyk, B.A., Aboudi, J. and Tang, T. (2007), "A critical evaluation of the predictive capabilities of various advanced micromechanics models", *Proceedings of the 48th Structures, Structural Dynamics, and Materials Conference*, Waikiki, Hawaii, April 23-26.